Astron. Astrophys. 298, 677–687 (1995)

ASTRONOMY AND ASTROPHYSICS

The gravitational wave sky

V.M. Lipunov[1,2], S.N. Nazin[2], I.E. Panchenko[2], K.A. Postnov[1,2], and M.E. Prokhorov[1]

[1] Sternberg Astronomical Institute, Moscow, 119899, Russia
[2] Faculty of Physics, Lomonossov University, Moscow, Russia

Received 13 July 1994 / Accepted 21 October 1993

Abstract. A view of the sky seen in gravitational waves in a wide frequency range $\sim 10^{-9} - 10^3$ Hz is considered. Stochastic gravitational wave background (GWB) produced by binary systems both galactic and extragalactic in origin is studied in more detail. A realistic "map" of the GW sky is constructed for the first time based on the observed stellar matter distribution within $\sim$ 50 Mpc from the Sun according to the Tully Catalog of Nearby Galaxies. This map accounts for both the binary produced stochastic GWB and GW radiated during supernova explosions. The total event rate of supernova explosions from the nearby galaxies is found to be about 40 per year. The coalescence rate of binary neutron stars in these galaxies is about 1 per year. We further study the "transparency" of the galactic stochastic GWB for observations made with GW detectors of different angular resolution. Critical frequencies above which the galactic and extragalactic GWB become transparent for a GW detector with 1° angular resolution were found to be about 2×10^{-3} Hz and $\sim$ 10 Hz, respectively.

Key words: gravitation – cosmology: miscellaneous – space vehicles

1. Introduction

The gravitational wave sky consists of several components different in their nature (see Grishchuk 1988; Thorne 1988 for a review). In view of future GW experiments which are under construction (LIGO, VIRGO – Abramovici et al. 1992; Thorne 1994) or under consideration (e.g. LISA mission, Danzmann et al. 1993), it is important to know what kind of astrophysical sources fall into the frequency range to be covered by these experiments ($\sim 10 - 1000$ Hz for LIGO/VIRGO $\sim 10^{-4} - 1$ Hz for LISA).

Galactic binary systems are known to produce a stochastic GW background (Lipunov et al. 1987; hereafter LPP87), as the number of binaries at each frequency interval $[\nu, \nu + d\nu]$ must be very high (typically, $10^6 - 10^9$ per frequency decade, see below). This background is spanned over more than 10 orders in frequency from 10^{-9} to 10^3 Hz. It was shown (Lipunov & Postnov 1987, 1988) that this stochastic background overlapped cosmological GW backgrounds which bear important information about the very early Universe (Grishchuk 1988) in a wide frequency range.

It is intuitively clear that at some frequency the GW-spectrum produced by binaries can stop being continuous, since at higher frequencies the evolution of a binary system is mostly controlled by orbital angular momentum removal by gravitational waves, rapidly increasing with frequency ($\dot{J}/J \propto \nu^{8/3}$), so that at some frequency less than one binary falls into the frequency interval at each moment. First studies of such spectra were performed by LPP87 and Hills et al. (1990).

These papers studied the GWB as seen by an all-sky GW detector. As the planned GW detector network can have a rather high angular resolution θ of about 1° (Thorne 1994), some questions concerning a more detailed structure of the binary produced GW background arise. Will it be possible to see "holes" in the galactic GWB by using a GW detector with high angular resolution? If yes, at what frequency and in what direction could this happen? What shall we see above these critical frequencies with our detector? Is there a possibility to "hunt" for cosmological GWBs, or this makes no sense? etc.

Putting aside the problem of detecting such stochastic signal, we will try to answer the above questions.

First, we consider properties of the galactic GWB; then we address to extragalactic GWB; at last, a realistic GWB and event rate contour maps are constructed for galaxies lying within a distance $\sim$ 50 Mpc from the Tully Catalog of Nearby Galaxies (Tully 1988).

2. Model of the Galaxy

2.1. Frequency distribution of galactic binaries

We assume galactic binary systems to be distributed uniformly in the logarithm of their semimajor axis A (Abt & Levy 1986),

$$d \log A = const \tag{1}$$

with minimal and maximal separations ranging from $A_{min} = 10R_\odot$ to $A_{max} = 10^7 R_\odot$. Equivalently, the frequencies of

gravitational waves emitted by these binaries, $\nu = 2\nu_{orb} = 1/\pi\sqrt{G(M_1+M_2)/A^3}$, initially occupy the frequency range $\sim 10^{-14} - 10^{-5}$ Hz.

Emission of gravitational waves makes the system shrink with time (on average), so that the blue end of the initial frequency distribution expands to higher frequencies. Theoretically, it can reach the frequency $\approx$ 1 kHz, corresponding to binary neutron star coalescence (see Fig.2.1).

As the observed distribution of binary periods is flat (cf. Eq. (1)), the normalization constant is the total number of galactic binaries $N_* = 10^{11} n_{11}$ per frequency decade:

$$F_0 = \frac{dN}{d\log\nu} = \frac{N_*}{\log \nu_{max}/\nu_{min}} \simeq \frac{1}{9}\cdot 10^{11} n_{11} \qquad (2)$$

It is clear that under a stationary star formation rate (which is a good approximation of the situation in our Galaxy) after some time the blue end of the GWB will be fully determined by coalescing binary white dwarfs (up to $\sim$ 1 Hz) and neutron stars (up to $\sim$ 1 kHz) (LPP87). The rate of frequency changing for coalescing binaries is

$$\dot{\nu} \approx (5.4\times 10^{-7}\mathrm{Hz/s})\mu\nu^{11/3},$$

where $\mu = m_1 m_2 m_\Sigma^{-1/3}$, m_1, m_2 are the masses of the binary components, and $m_\Sigma = m_1 + m_2$ is the total mass expressed in Solar units. The stationary continuity equation provides us with spectral density of the number of stars

$$\frac{dN}{d\nu} \equiv N_\nu = \frac{f}{\dot{\nu}} \simeq (6\cdot 10^{-4}\mathrm{Hz}^{-1})\frac{f_{100}}{\mu}\nu^{-11/3}, \qquad (3)$$

where f is a coalescence rate of the binaries, $f_{100} \equiv f/(0.01\mathrm{yr}^{-1})$. Then the number of stars per decade is

$$\frac{dN}{d\log\nu} = \frac{N_\nu \nu}{\log e} = 1.4\times 10^{-3}\frac{f_{100}}{\mu}\nu^{-8/3}. \qquad (4)$$

The red end of the GWB will not change and a characteristic "break" will appear in the spectrum. This break occurs at the frequency ν_b defined by the matching condition

$$\left.\frac{dN}{d\log\nu}\right|_{red} = \left.\frac{dN}{d\log\nu}\right|_{blue}, \qquad (5)$$

from which one finds

$$\nu_b \approx (10^{-5}\mathrm{Hz})\left(\frac{f_{100}}{\mu}\right)^{3/8}. \qquad (6)$$

This distribution will hold up to a frequency of about $\nu_1 \approx 1$ Hz corresponding to the limiting frequency of binary white dwarfs. Only the binary neutron stars or black holes will form the blue end of the distribution up to $\sim$ 1 kHz. Thus the resulting form of the distribution is:

$$f(\log\nu) = \begin{cases} F_0, & \nu < \nu_b \\ F_0(\nu/\nu_b)^{-8/3}, & \nu_b < \nu < \nu_1 \\ F_0(\nu/\nu_1)^{-8/3}(N_{ns}/N_*), & \nu > \nu_1 \end{cases} \qquad (7)$$

These simple qualitative considerations are fully consistent with results from numerical calculations (see Fig. 1).

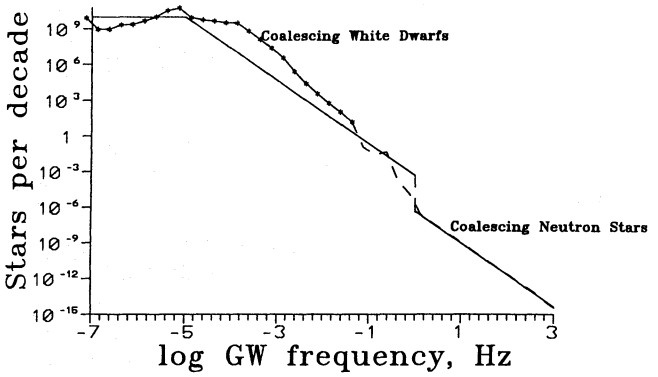

Fig. 1. Number of binary stars per frequency decade. The total number of stars in the Galaxy is 10^{11}. Numbers < 1 are mathematical expectations. Analytical estimation (7) is shown by the solid line

Table 1. The model components of the Galaxy

Component	a_0,kpc	M_{10}	ε
Nucleus	0.005	0.009	0.6
Bulge	0.2	0.45	0.6
Halo	2	1.2	0.3
Disk	4.6	7.7	0.1
Flat comp.	6.4	1.0	0.02
Corona	75	110	1

2.2. Structure of the Galaxy

One of the most detailed models of the structure of our Galaxy has been developed by Einasto (1979). It involves 6 components: nucleus, bulge, halo, disk, flat component and corona (see Table 1).

The parameters of the model resulted from a numerical fitting of various data, such as the observed distribution of young star population and neutral hydrogen, the density of population II stars in the vicinity of the Sun, the galactic rotation curve and the dynamics and distribution of globular clusters and dwarf irregular satellites of the Galaxy.

In Table 1 a_0 is the semimajor axis of an ellipsoid representing each component; M_{10} is the mass of each component in units of 10^{10} solar masses; ε is the flatness of the ellipsoid. The density of matter in the Galaxy is expressed as

$$n(r,z) = \sum_{i=1}^{6}\frac{M_i\varepsilon}{2\pi a_0^3}\exp(-r/a_0 - |z|/(\varepsilon a_0)) \qquad (8)$$

where r is the distance from the galactic center, z is the distance from the galactic plane.

Note that the huge mass of the corona that is evidenced by the motion of the dwarf satellites of the Galaxy, can hardly be fully comprised in stars. The fraction of stars in the corona is an important parameter for the models of gravitational radiation of the Galaxy: its variation would cause a significant change of gravitational radiation from the galactic polar regions, which is mostly populated by the stars from the galactic corona.

In this paper the fraction of stars in the corona is assumed to be $\kappa = 10\%$. We note that future gravitational wave observations could help to determine the value of κ.

3. Transparency of the stochastic background

We will call "transparency" of the background the ability of the observer to detect gravitational wave signals other than those produced by binary systems, by varying parameters of the used gravitational wave detector (namely, its angular resolution and frequency band), so that less than one occasional binary system falls into the detector's beam at a given frequency in a given direction.

3.1. Galactic GWB

Let the sky be observed with a detector having a pencil beam diagram 2θ across. The number of stars per frequency decade that is sweeped by the detector is a function of celestial coordinates (say, galactic coordinates l, b):

$$N_\theta(l,b) = \int_{\pi\theta^2} \int_{\log\nu}^{\log\nu+\Delta\log\nu} \frac{dN}{d\log\nu d\Omega}(l,b) d\Omega\, d\log\nu\,. \tag{9}$$

For a homogeneous distribution of stars over the sky this number is coordinate independent:

$$N_\theta = \frac{\theta^2}{4} \int_{\log\nu}^{\log\nu+\Delta\log\nu} \frac{dN}{d\log\nu} d\log\nu\,. \tag{10}$$

Here θ is defined as

$$\theta = \frac{1}{\pi}\sqrt{\Omega} \tag{11}$$

i.e. the entire sky (4π steradian) corresponds to $\theta = 2$, and for small θ this is just the halfwidth of the beam.

The background becomes transparent once $N_\theta(\theta_{cr}) < 1$; this inequality provides us with a critical angular resolution $\theta_{cr}(l,b)$ the detector should have not to "notice" the background. For obtaining rough estimates we can use a "homogeneous" galaxy to find

$$\theta_{cr} \approx 4'' \begin{cases} C_0^{-1/2} n_{11}^{-1/2}, \\ \quad \text{for the red branch,} \\ \quad \nu < \nu_b, \\ C_{-8/3}^{-1/2} \left(\dfrac{\mu}{f_{100}}\right)^{1/2} \left(\dfrac{\nu}{\nu_b}\right)^{4/3}, \\ \quad \text{for the blue branch,} \\ \quad \nu > \nu_b. \end{cases} \tag{12}$$

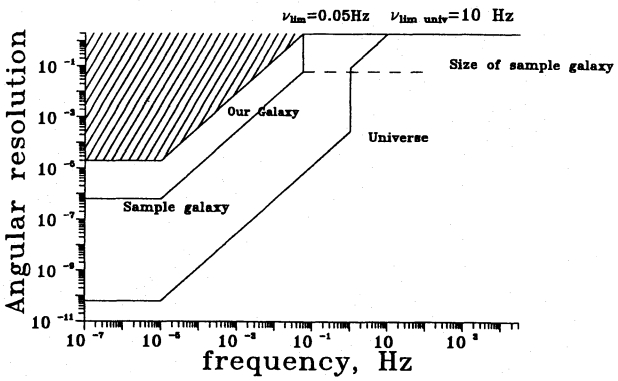

Fig. 2. The regions of transparency of the GWB from different objects in the angular resolution of the detector – critical frequency ν_{cr} diagram. The GWB from a homogeneous model of our Galaxy (the total number of stars is 10^{11}) is transparent below the line labelled as "Our Galaxy". The line marked as "Sample galaxy" shows the transparency boundary for a Milky Way-type galaxy with observed angular size $\simeq 8°$. The break at 0.05 Hz is caused by continuity limit of the binary white dwarfs merging at a rate of 1 per 100 yr. The bottom curve shows the tranparency boundary for the GWB from 10^{11} external galaxies. The upper horizontal line corresponds to an all-sky detector ($\theta = 2$). The hatched region corresponds to the "absolute hopeless"

The numerical factor $C_\alpha(\Delta\log\nu)$ denotes

$$C_\alpha(\Delta\log\nu) = \nu^{-\alpha} \int_{\log\nu}^{\log\nu+\Delta\log\nu} \nu^\alpha d\log\nu = \frac{\log e}{\alpha}\nu^\alpha \left(10^{\alpha\Delta\log\nu} - 1\right) \tag{13}$$

and

$$C_\alpha(\Delta\log\nu) \to \Delta\log\nu\,, \quad \text{if } \alpha \to 0 \text{ or } \Delta\log\nu \to 0 \tag{14}$$

(below the dependence $(\Delta\log\nu)$ will be omitted). Obviously, the red part is of no interest (unless one observes a region of the sky which is very poor in stars), and for the blue part one finds a critical frequency, ν_{cr}, above which no stars occur in the region of the sky subtended by the detector's beam. The function $\theta\nu$ is shown in Fig. 2.

It is clear from the figure that for an all-sky detector the Galaxy becomes transparent above the frequency $\nu_{cr} \simeq 0.05$ Hz. For realistic detectors in the LIGO network with angular resolution of about 1° this frequency reduces to $\sim 2 \times 10^{-3}$ Hz.

The isolines of the critical frequency on the (l,b) sky map are presented in Fig. 3.for the galactic model described above with 10% of the mass of the corona consisting of stars, as seen by the 1°-detector.

3.2. Extragalactic GWB

The general shape of the GWB formed by extragalactic binaries was considered in earlier works (LPP 1987, Hills et al. 1990).

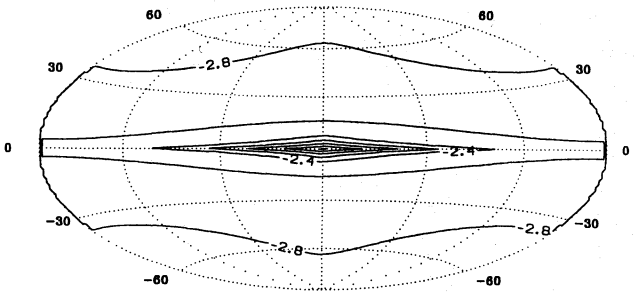

Fig. 3. Isolines of the critical frequency on the (l, b)-sky map for the model of the Galaxy described in the text

Now we turn to the question how the GWB changes if one makes observations with a GW detector with angular resolution θ. It is intuitively clear that at frequencies above the critical ones for our Galaxy, one will detect rare bright jerks produced by coalescing white dwarfs (at a rate of ~ 1 per 100 yr) and neutron stars (at a rate of ~ 1 per a few 10 thousands yr) in our Galaxy, against a background of the extragalactic stochastic GW. In analogy to our Galaxy, critical frequencies must exist for the extragalactic background. Above them only merging neutron stars will cross a given frequency interval at a rate of up to $\sim 30-100$ per yr if one observes all galaxies within 200 Mpc. Firstly we consider GWB from close individual galaxies, and then will discuss overall extragalactic GWB. The same questions as for the Milky Way galaxy are addressed.

3.2.1. GWB from individual galaxies

The number of binaries per frequency decade per solid angle from a separate stellar system (galaxy or cluster of galaxies) is

$$\left.\frac{dN}{d\log\nu d\Omega}\right|_{ext} = \left.\frac{dN}{d\log\nu d\Omega}\right|_{Gal}\left(\frac{4}{\theta_e^2}\right)\left(\frac{n_{11\,e}}{n_{11}}\right), \tag{15}$$

where θ_e is the angular size of the object, $n_{11\,e}$ is the total number of stars in this object, which is assumed to be homogeneous in surface density. For example, for the Andromeda galaxy M31 ($\theta \sim 1/30$rad, $n_{11\,e}/n_{11} = 1$) one gets

$$\left.\frac{dN}{d\log\nu d\Omega}\right|_{And} \sim 4000\ \left.\frac{dN}{d\log\nu d\Omega}\right|_{Gal} \tag{16}$$

therefore $\theta_{cr}(\nu)|_{And} \simeq 1/60\,\theta_{cr}(\nu)|_{Gal}$ (see Eq. (12)). The detector's beam halfwidth as a function of frequency is shown in Fig. 3. If the angular size of the galaxy is less than the angular resolution of the detector, the critical frequency is independent of the angular resolution,

$$\nu_{cr}(\theta)|_{\theta_{ext}<\theta} = \nu_{cr}(2)|_{ourGalaxy} \tag{17}$$

3.2.2. Critical frequencies and GW detector's halfwidth for extragalactic GWB observations

To get rid of the extragalactic GWB produced by binaries, one can use the above considerations to find the optimal detector halfwidth and frequency for observations. Again, for simple estimates we can suppose the stars in the Universe to be distributed homogeneously. Assuming an average galaxy to consist of 10^{11} stars and the total number of galaxies in the Universe to be $10^{11}N_{11}$, we get the average number of stars per decade falling into the detector's beam to be

$$N_{\theta\,e} = C_0\left(\frac{1}{9}10^{11}n_{11}\right)10^{11}N_{11}\frac{\theta^2}{4} \tag{18}$$

for the flat red end of the GWB, and

$$N_{\theta\,e} \simeq 3.5\times10^7 C_{-8/3}\frac{f_{100}N_{11}}{\mu}\theta^2\nu^{-8/3} \tag{19}$$

for the blue end of the GWB formed by coalescing binaries. Equating $N_{\theta\,e}$ to unity, one finds the critical detector's halfwidth

$$\theta_{cr\,e} \approx \begin{cases} 10^{-5''}\,C_0^{-1/2}(n_{11}N_{11})^{-1/2}, \\ \quad \text{for the red branch,} \\ \quad \nu < \nu_b, \\ \\ 36''C_{-8/3}^{-1/2}\left(\dfrac{\mu}{f_{100}N_{11}}\right)^{1/2}\nu^{4/3}, \\ \quad \text{for the blue branch,} \\ \quad \nu > \nu_b. \end{cases} \tag{20}$$

One immediately notes that observations at low frequencies ($\nu < \nu_b$) are always contaminated by the stochastic binary GWB. In contrast, by observing the sky with a GW detector having narrow enough halfwidth $\theta < \theta_{cr\,e}$, one will not "see" the extragalactic GWB at frequencies $\nu > \nu_b$.

Alternatively, if one uses a GW-detector with a fixed halfwidth of the beam, Eq. (20) gives the answer to the question at what frequency one should make observations to have no binary produced stochastic noise. In fact, the transparency of the extragalactic GWB occurs at frequencies above 1 Hz, that is in the part of the spectrum produced by coalescing binary neutron stars. Taking for their rate $f_{100} = 0.01$, one finds that the extragalactic GWB begins to be transparent above the frequency

$$\begin{aligned}\nu_{lim} &= \left(6.2\times10^6 C_{-8/3}\frac{f_{10000}N_{11}}{\mu}\theta^2\right)^{3/8} \\ &\approx (6\text{Hz})\left(C_{-8/3}\frac{f_{10000}N_{11}}{\mu}\right)^{3/8}\left(\frac{\theta}{1\text{deg}}\right)^{3/4}\end{aligned} \tag{21}$$

(cf. Fig. 3).

4. Amplitude distribution

In this section we consider the GWB spectrum as such, that is we study how the dimensionless strain metric amplitude h depends on frequency. For a sample of N independent binaries emitting GW at a given frequency ν the net result is

$$h(\nu)_\Sigma = \sqrt{\sum_i h_i^2(\nu)}\,. \tag{22}$$

If one uses the frequency interval $d\log\nu$, the result will be

$$\langle h(\nu)\rangle = \left(\int_{\log\nu}^{\log\nu+\Delta\log\nu} \frac{dN}{d\log\nu} d\log\nu h_1^2(\nu, r_{eff}, m_{eff}) \right)^{1/2},$$

where

$$h_1(\nu, r, m) \simeq 4.4\times10^{-20}\mu\nu^{2/3}\left(\frac{1\text{kpc}}{r}\right) \quad (23)$$

is the familiar amplitude produced by an individual binary, r_{eff} and m_{eff} are the effective distance to the sample and the effective mass of the binaries (in solar units) producing the GW radiation at the frequency ν. For example, for a homogeneous sample (which is a good approximation to extragalactic binaries) one obtains $r_{eff} = 1/\sqrt{3}R_{max}$, where R_{max} is the outer boundary of the sample.

Making use of expressions (2), (4) and (23) yeilds

$$\langle h\rangle|_r \approx 4.4\times10^{-15}C_{4/3}^{1/2}\mu\left(\frac{1\text{kpc}}{r_{eff}}\right)\nu^{2/3}, \quad (24)$$

for the red part of the spectrum ($\nu < \nu_b$), and

$$\langle h\rangle|_b \approx 1.6\times10^{-21}(\mu f_{100}C_{-4/3})^{1/2}\left(\frac{1\text{kpc}}{r_{eff}}\right)\nu^{-2/3}, \quad (25)$$

for the blue end.

One may be interested in how the GWB from the external object relates to that from our Galaxy, provided that the observations are being performed with a detector of angular resolution $\theta > \theta_{cr}(\nu)$ such that the Galaxy is still not transparent at the frequency of observations, and the object is inside the detector's beam, $\theta_{ext} < \theta$. In this case

$$\frac{\langle h\rangle|_{ext}}{\langle h\rangle|_{ourGal}} = \left(\frac{n_{ext}}{n_G}\right)^{1/2}\left(\frac{r_{ext}}{r_G}\right)^{-1}\left(\frac{\theta_{ext}}{2}\right)^{-1}$$

Here n_{ext} is the number of stars in the object, r_G is an effective "radius" of the Galaxy, $r_G \sim 7$ kpc. Some specific examples are shown in Table 2.

It is seen from the Table 4 that only the closest stellar systems (such as the Magellanic Clouds and M31) can noticeably influence the galactic binary background. The level of the cosmological binary GWB is always an order of magnitude below the galactic one. Indeed, by analogy with expressions (24) and (25) one gets for the red (flat) and blue (decreasing) parts of the spectrum, respectively:

$$\langle h\rangle|_r = 2.1\times10^{-16}C_{4/3}^{1/2}\mu\sqrt{n_{11}N_{11}}\left(\frac{3500\text{Mpc}}{r_{eff}}\right)\nu^{2/3},$$

$$\langle h\rangle|_b = 1.4\times10^{-22}C_{-4/3}^{1/2}\sqrt{\mu f_{100}N_{11}}\left(\frac{3500\text{Mpc}}{r_{eff}}\right)\nu^{-2/3}.$$

Their comparison with expressions (24) and (25) yields $\langle h_{cosmol}\rangle/\langle h_{Gal}\rangle \sim 1/20$ for both ends of the spectrum. Note that our definition of the stochastic strain amplitude $\sqrt{4\pi}$ times higher the characteristic amplitude h_c introduced by Thorne (1988).

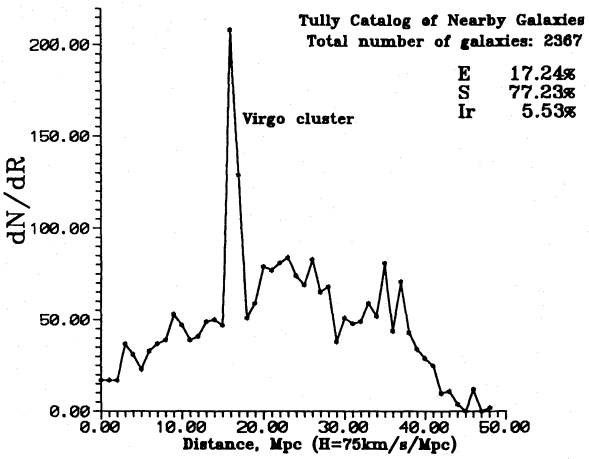

Fig. 4. Distribution of galaxies from Tully Catalog by distance

Energy density of the stochastic GWB per unit logarithmic interval of frequency divided by the critical energy density $\rho_{crit}c^2 \approx 3\times10^{-8}(H_0/100\text{km/s/Mpc})^2$ ergs/cm^3 to close the Universe is

$$\Omega_{GW}(\nu) \simeq 5.3\times10^{-11}h_{100}^{-2}\left(\frac{3500\text{Mpc}}{r_{eff}}\right)^2 \times \mu^{3/4}f_{100}^{5/4}n_{11}^{-1/4}N_{11}C_{-4/3}^{5/4}C_{4/3}^{-1/4}\begin{cases}\left(\frac{\nu}{\nu_0}\right)^{10/3}\\ \left(\frac{\nu}{\nu_0}\right)^{2/3}\end{cases} \quad (26)$$

Here the characteristic frequency

$$\nu_0 = 1.3\times10^{-5}\text{ Hz}\left(\frac{f_{100}}{\mu n_{11}}\right)^{3/8}\left(\frac{C_{-4/3}}{C_{4/3}}\right)^{3/8} \quad (27)$$

is close to the break frequency ν_b (6).

The GW noise produced by extragalactic binary systems is still considerably higher than the expected amplitudes of relic gravitational waves produced in popular inflationary models (e.g. Rubakov et al. 1982): $h(\nu) \le 10^{-25}/\nu$ (observational estimation is $\Omega_g \le (\Delta T/T)^2 \simeq 10^{-11}$, see Smoot 1992; Strukov et al. 1993), even if one makes observations at the galactic poles where one has fewer stars.

5. A GW map of nearby galaxies

In this section we will discuss the view of the GW sky above the critical frequency of transparency of the stochastic background. At these frequencies only rapidly rotating neutron stars can generate the periodical GW signal (Thorne 1988), binary neutron stars mergers and supernova explosions produce burst-like GW. No reliable estimates of the number of rapidly rotating neutron stars can be obtained at the moment. However, one can estimate the event rates of supernova explosions and binary neutron star

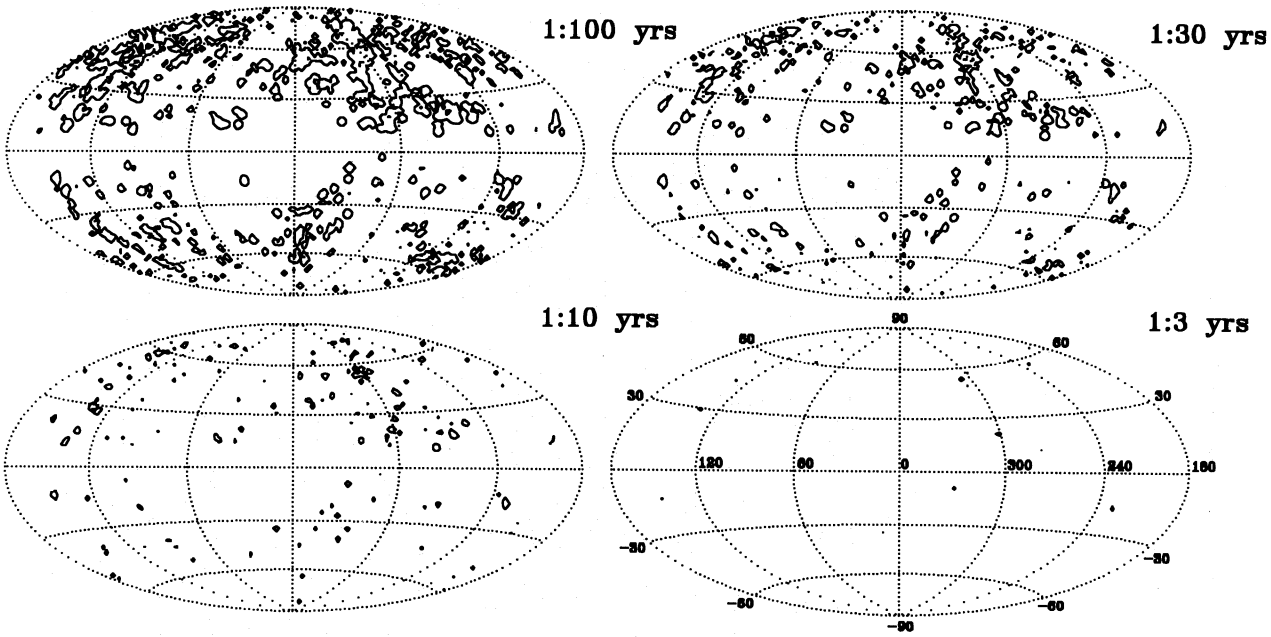

Fig. 5. The sky distribution of the total supernova frequency from nearby galaxies in terms of lines of equal frequencies per square degree. The total SN frequency exceeds 1 per 3, 10, 30 and 100 yr per square degree inside the encircled regions

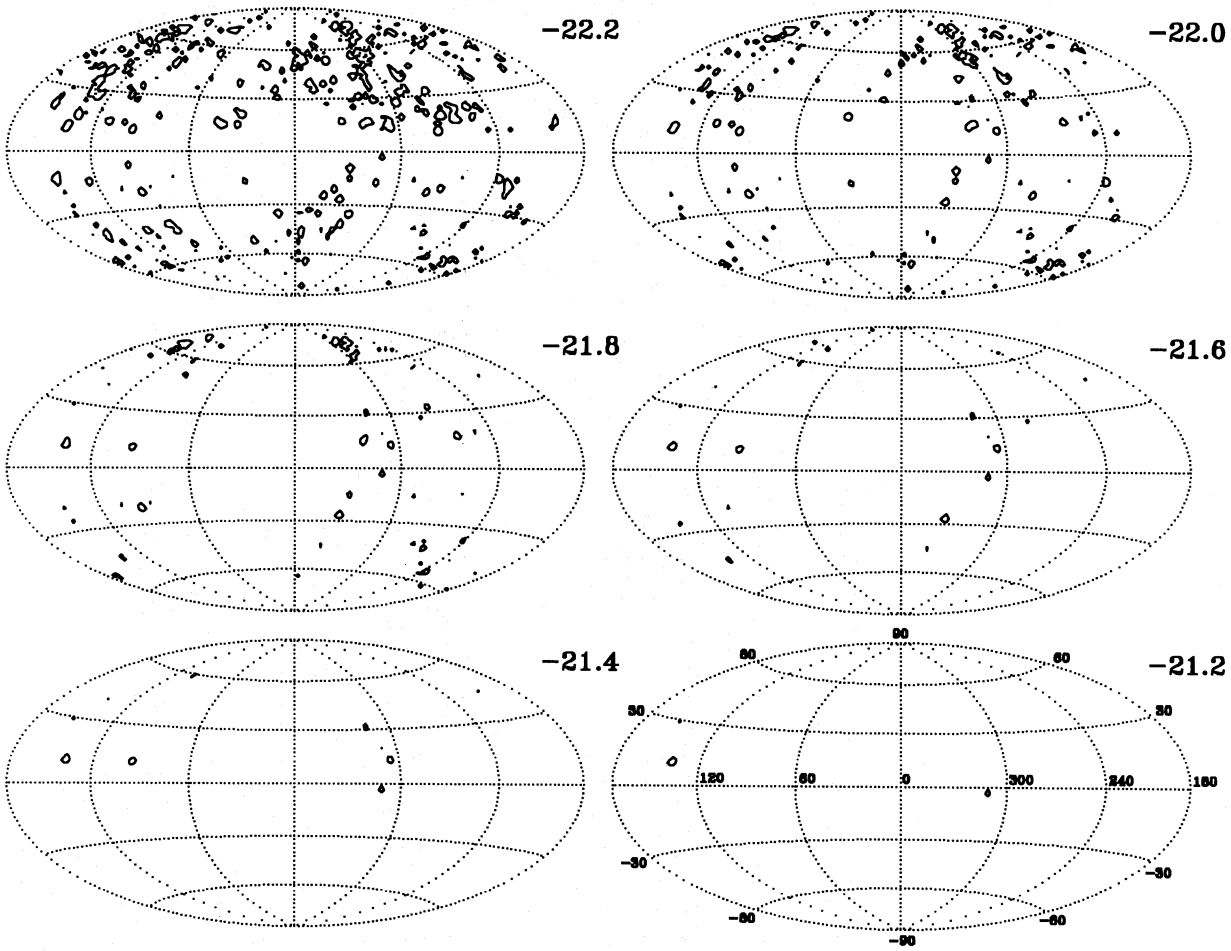

Fig. 6. Distribution of GW amplitudes from SN events over the sky. Inside the encircled areas the total SN event rate $> 1/(30\mathrm{yr})/\mathrm{deg}^2$ at a given level of h_c

Table 2.

Object	Number of stars, 10^{11}	Effective distance, r_{eff}	Angular size, θ_{ext}	$\frac{\langle h\rangle\|_{ext}}{\langle h\rangle\|_{ourGal}}$
Milky Way	~ 1	~ 7 kpc	2	1
LMC	~ 0.1	55 kpc	$230' \sim 1/7$	~ 1
M31	~ 1	~ 600 kpc	$1^\circ \sim 1/57$	~ 1
Virgo Cluster	$\sim 10^3$	~ 15 Mpc	$\sim 6^\circ \sim 1/10$	0.2
All Universe	$\sim 10^{11}$	~ 3500 Mpc ($R_{Hubble} \sim 6000$ Mpc)	2	~ 0.6

coalescences by using current astronomical observations and theoretical predictions and the observed distribution of matter in the vicinity of our Galaxy. As the closest GW sources are the strongest ones, we will consider Tully's Nearby Galaxies Catalog (Tully 1988) comprising 2367 galaxies from a sphere of $\sim$ 50 Mpc in radius. The luminosities are unknown for 596 of these galaxies, so that they cannot be included in the analysis. This catalog is almost complete up to distances of $\sim$ 30 Mpc (Fig. 4).

5.1. GW from supernova explosions

The observed supernova frequencies of different types (SN Ia, Ib, II) in different types of galaxies (E–...–S–...–Ir) (see van den Bergh & Tammann 1991) immediately provide us with the SN frequency distribution in space. We can investigate projection of this distribution onto the selectial sphere in two ways: in terms of lines of constant SN frequencies per square degree for all galaxies from the sample (Fig. 5), and in terms of constant GW amplitudes at a given SN frequency per square degree (Fig. 6).

We use after Thorne (1988) the characteristic strain metric amplitude h_c to be:

$$h_c = 2.7 \times 10^{-22} \left(\frac{\Delta E_{GW}}{10^{-4} M_\odot c^2}\right)^{1/2} \left(\frac{1kHz}{f_c}\right)^{1/2} \left(\frac{10Mpc}{r_0}\right)$$

where r_0 is a distance to the source, ΔE_{GW} is the total energy radiated as GW; a very optimistic estimate of the GW energy during a SN explosion of $\sim$ 0.1% of the expected neutrino luminosity is used. Characteristic frequency of the GW burst is assumed to be 1 kHz. We must note that GW bursts produced by supernova explosions have been poorly understood so far, so only relative figures of h_c may have a meaning.

Inside regions encircled by the lines of constant SN frequency in Fig. 5, the total SN frequency exceeds 1 per 3, 10, 30 and 100 yr per a square degree, respectively. This figure represents the cross-sections of the projected mass density per a square degree by mass.

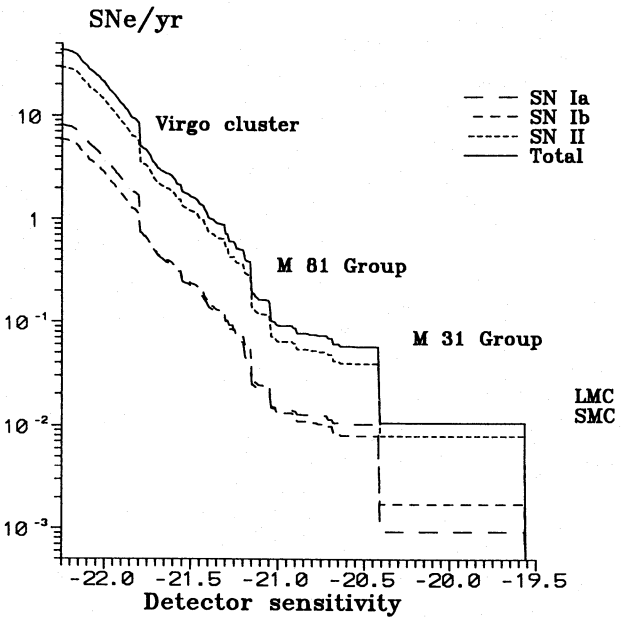

Fig. 7. SN rates of different types integrated over the whole sky as a function of a given detector sensitivity in terms of the strain metric amplitude h_c. Contributions from some close groups of galaxies are indicated

Inside regions encircled by the lines of constant h_c (Fig. 6), the total SN event rate exceeds $1/(30\text{yr})/\text{deg}^2$ at a given level of h_c. In other terms, these lines represent cross-sections of nearby galaxy space distribution by distance.

In Fig. 7 the SN rates of different types integrated over the whole sky are plotted as a function of a given detector sensitivity in terms of the strain metric amplitude h_c. Clearly seen are contributions from the closest groups of galaxies and the Virgo cluster (assuming a Hubble constant of 75 km/s/Mpc). At better sensitivities ($h_c < 10^{-21.2}$) a power law with a slope of -3 is seen, $N(h) \propto h^{-3}$, which reflects the nearly isotropical

distribution of matter beyond $\sim$ 7 Mpc. The total rate of SN events over the sky for nearby galaxies is about 40 per year.

5.2. GW from coalescing compact binary stars

The GW from coalescing compact binaries composed of neutron stars and black holes are the best understood of all astrophysical GW sources. A conservative lower limit to the event rate of galactic binary neutron star coalescence of about 1 per $\sim$ 100,000 yr follows from studies of double pulsar statistics (Narayan et al. 1991; Phinney 1991). Theoretical estimates, however, give much higher values, of about 1 per $\sim$ 10,000 yr (LPP87; Tutukov & Yungelson 1993). Observational estimates are subjected to (unknown) selection effects, whereas theoretical estimates based on evolutionary studies of binary stars use a number of poorly known parameters of binary evolution, such as the initial binary mass distribution exponent α_q ($f(q = M_2/M_1) \propto q^{\alpha_q}$, where $M_1 > M_2$ are the initial masses of the binary components), and common envelope stage efficiency α_{CE} that determines to what extent the binary shrinks during the common envelope stage (see van den Heuvel (1994) for further details about evolutionary scenarios). Essentially, the discrepancy between the statistical and theoretical estimations is connected with the fact that many close binary old neutron stars cannot be already observed as radiopulsars (see also discussion in van den Heuvel 1994).

Recently Lipunov et al. (1994) made extensive numerical simulations of the binary star evolution in the Galaxy using a "Scenario Machine" – a computer code that incorporates all current ideas about the evolution of both normal and magnetized rotating compact stars (white dwarfs, neutron stars, black holes) in binaries and permits one to model the galactic binary population according to different evolutionary scenarios. By comparing the resulting "view" of the model galaxy with observations, they showed that the best values of the key scenario parameters mostly compatible with the observed numbers of galactic X-ray sources of different kinds, cataclysmic variables and ratios of pulsars with different binary companions, are $\alpha_q \simeq 2$ and $\alpha_{CE} \simeq 0.5$.

In Fig. 8 we show the rates of coalescence of binary white dwarfs and neutron stars in a model elliptical galaxy with a mass of $10^{11} M_\odot$, depending on the time elapsed since the (assumed instantaneous) star formation. Calculations were made with the adopted best values of key evolutionary parameters (Lipunov et al. 1994). A solar chemical abundance was assumed. We assumed the conservative orbital evolution during the mass transfer process, and the common envelope stage creation was assumed to begin once a fast (on the thermal or shorter time-scale of the Roche-filling component) mass transfer occurs in a binary with a certain mass ratio depending on the evolutionary states of the binary components (see Webbink 1979). We note that the coalescence rate of double white dwarfs one per a few 100 yr depends only slightly on the parameters, making these events an attractive mechanism for supernova type 1a observed in elliptical galaxies at nearly the same rates (Iben & Tutukov 1984). The evolution of supernova rates in elliptical galaxies was first

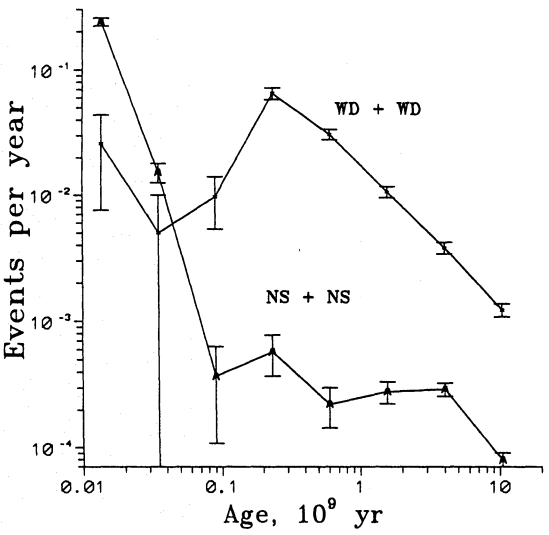

Fig. 8. Evolution of the coalescence rates of WD+WD (with $m_1 + m_2$ over the Chandrasekhar limit) and NS+NS binaries with time in a model elliptical galaxy with a mass of $10^{11} M_\odot$

modelled by Lipunov & Postnov (1988). Unlike to double white dwarfs, the coalescence rate of double neutron stars evolves significantly with time and practically vanishes after about 7 billion years of galactic evolution.

Having calculated the evolution of binaries in the model elliptical galaxy with a δ-function-like star formation, one can easily model the evolution of a galaxy with an arbitrary time dependence of the star formation rate. For example, a normal spiral galaxy can be approximated as having a constant star formation rate. In this case, our calculations give a coalescence rate of double neutron star once per $\sim$ 4,000 yr.

The next obvious step was to calculate the distribution of the binary neutron star coalescence event rates on the sky, using Tully Catalog of Nearby Galaxies. Since nothing is known about initial binary distributions in other galaxies, we have assumed that an initial mass function $f(m_1, m_2) = f(m_1) \cdot f(q)$ of binary components and initial semimajor axes distribution $f(a)$ of binaries in all galaxies similar to that observed in our Galaxy:

$f(m_1) \propto m_1^{-2.35}$, $\quad 0.8 < m_1 < 120 M_\odot$
(Salpeter mass function)
$f(q) \propto q^2$, $\quad 0.01 < q < 100$
$df(a) \propto d \log(a)$, $\quad$ (Abt & Levy 1976).

The total number of binaries in a galaxy must be proportional to its total mass, which can be estimated by using an average mass-luminosity relation for galaxies of different morphological types. We adopted the M/L relation following Sil'chenko (1984):

These values give estimations of the mass of the stellar content of galaxies (dark matter halo is not included) to an accuracy of factor 2.

Star formation rates were taken to be constant for both spiral and irregular galaxies; for elliptical galaxies the star formation rate was assumed to be constant and nonzero only during the first billion years.

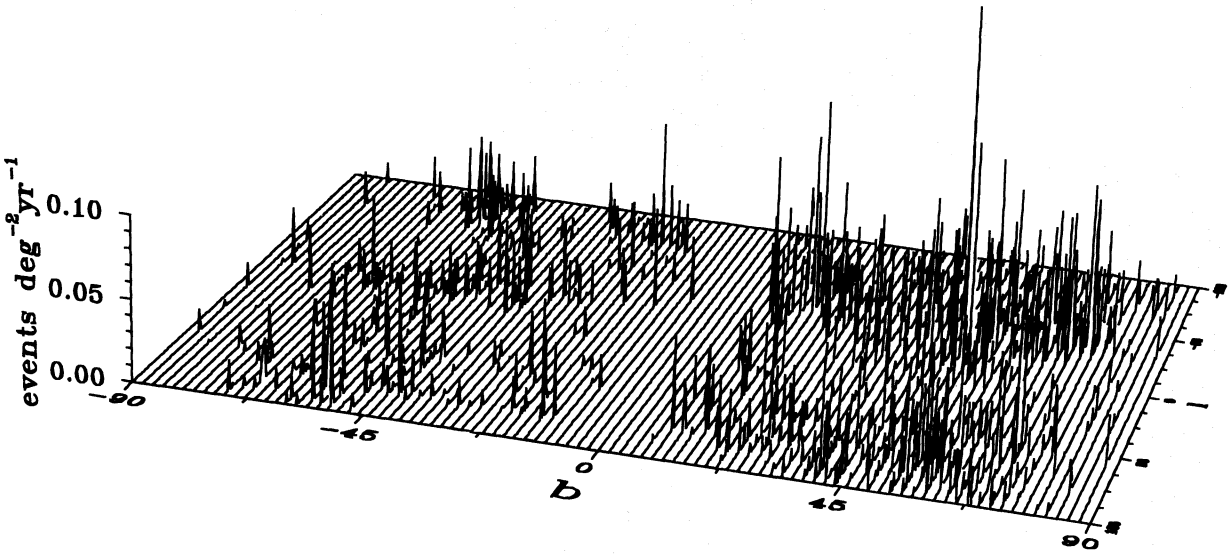

Fig. 9. Coalescence rate of the binary neutron stars in terms of events per one square degree per year in the galactic coordinates l, b. The total event rate is $\sim$ 3 events per year

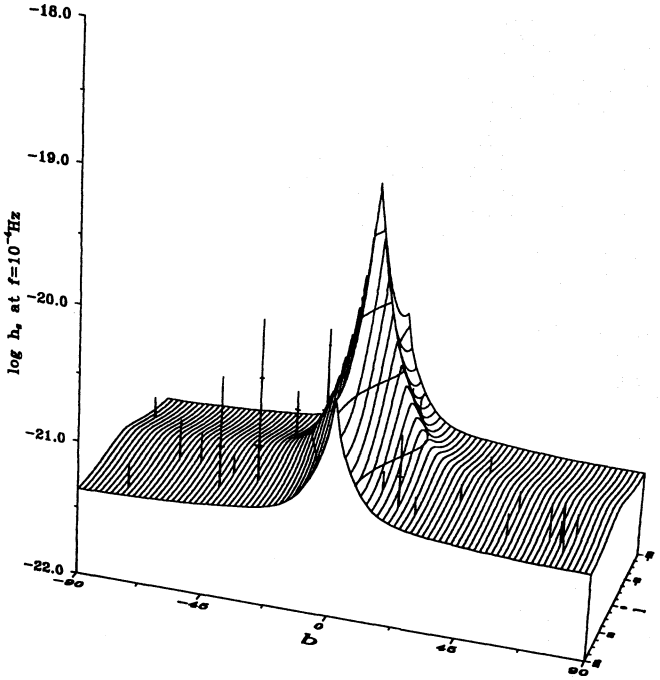

Fig. 10. Stochastic GWB produced by binaries from Tully's catalog against the GWB from our Galaxy at the frequency 10^{-4} Hz, in terms of the mean strain metric amplitude per square degree in a given direction

The resulting map of coalescence rate of binary neutron stars is shown in Fig. 9 in terms of events per one square degree per year. The event rate integrated over the whole sky is $\sim$ 1 per year. As optical Tully's catalogue underestimates the number of galaxies (for example, due to absorption in the Milky Way plane), this is a very promising estimate for the LIGO experiment.

Table 3.

Morfological type	M/L (in solar units)
E	10
Sa...Sb	4...5
Sc, Ir	2

5.3. GWB from nearby galaxies

The stochastic binary background produced by nearby galaxies from Tully's catalog at the frequency 10^{-4} Hz is shown in Fig. 10 in terms of the average strain metric amplitude per square degree in a given direction (l, b) on the sky:

$$h_s^2 = \int_{\nu}^{\nu+\Delta\nu} \sum_{sources} h_i^2 d\log\nu$$

where the sum is calculated over all sources in the given square degree of the sky; we assumed $\Delta\nu = \nu$.

The lines of constant h_s on the sky (so-called "isograwes") are plotted in Fig. 11. As we expected (see Sect. 4), only the closest and the most massive galaxies (such as SMC, LMC, M31, M82, M87) can be clearly discerned by a GW detector with an angular resolution of 1 degree against the galactic binary GW stochastic background. .

6. Conclusions

For the first time, an expected map of the sky in gravitational radiation has been constructed on the basis of the observed stellar matter distribution within 50 Mpc distance from the Sun. As the input data for the study Tully's Catalog of Nearby Galaxies has been used. The expected gravitational wave sources taken into

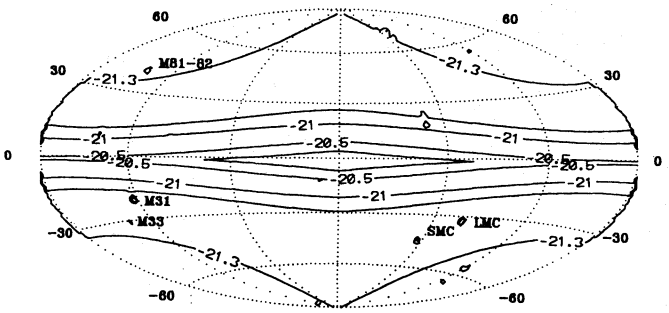

Fig. 11. The "isograwes" from Fig. 10 projected onto (l, b)-plane

account include binary stars and supernova explosions. The results are given separately for galactic and extragalactic sources and are compared with the planned sensitivity and angular resolution of the ground based and spaceborn laser interferometer gravitational wave detectors. In particular, it was studied under which conditions the gravitational wave background (noise) produced by binary stars in our Galaxy becomes transparent for observations of the extragalactic sources. The principal conclusions are listed below.

i) Galactic gravitational wave background

It is shown that the stochastic gravitational wave background produced by binary systems in our Galaxy has an increasing power spectrum with a slope of (2/3) at frequencies below approximately 10^{-5} Hz. For higher frequencies, the spectrum decreases as the (-2/3) power of frequency. The spectrum ceases to be continuous at frequencies of the order of 1 Hz where the number of sources becomes small and their signals do not overlap. In the interval 1 Hz – 1 kHz, only individual binaries consisting of neutron stars and/or black holes can contribute to the gravitational wave emission of the Galaxy. For the LIGO/VIRGO gravitational detectors with a resolution of the order of one angular degree, the galactic background becomes transparent at frequencies higher than 10^{-3} Hz.

ii) Extragalactic gravitational wave background

It is found that the closest and the biggest stellar systems, such as the Magellanic Clouds, M31, M82, M87, can significantly alter the level of the background radiation generated by the Galactic binaries. The level of the background produced by binaries located in galaxies at much larger distancies is about one order of magnitude smaller than the Galactic background. However, this level is still considerably higher than the expected amplitudes of relic gravitational waves produced in certain currently popular inflationary models. This can make the observations of relic gravitational waves very difficult (in this frequency interval) unless the difference in the statistical properties of the two types of signals is somehow exploited.

iii) Gravitational wave map of nearby galaxies

Tully's catalog has been used in order to evaluate the expected distribution in space of supernova explosions and compact binary coalescences as sources of gravitational radiation. The event rate of supernova explosions has been evaluated on the basis of the observed rates for type Ia, Ib, II supernovae in galaxies of various types. The spatial distribution has been projected onto the celestial sphere in terms of lines of constant supernova rate per a square degree and in terms of lines of constant gravitational wave amplitude for a given supernova rate per a square degree. The total event rate for galaxies from the catalog is about 40 per year.

The estimate of the event rate for the neutron star coalescences has been revised on the basis of evolutionary tracks with the corrected values of parameters describing the initial mass distribution and common envelope stage. The derived event rate is about one per $\sim 4,000$ years per $10^{12} M_{\odot}$ which is significantly higher than the previously published estimates (one per 100,000 years) based on binary pulsar statistics only. This encouraging result may be important for correcting the strategies of observations in the LIGO/VIRGO experiments.

Acknowledgements. The authors especially acknowledge Prof. L.P. Grishchuk for formulating the problem and enlightening discussions; we also thank Profs. D.A. Varshalovich, D.G. Yakovlev and M.V. Sazhin for useful and stimulating discussions. KAP thanks the ISF Travel Grant Program for financial support. The work was partially supported by the ESO C&EE Programme Grant No A-02-079 and RFFI Grant No 94-02-04049a.

References

Abramovici, A. et al. 1992, Sci. 256, 325.
Abt, H. & Levy, S.G. 1976, ApJSS 36, 241.
Danzmann, K., Rüdiger, A., Schilling, R., et al. 1993, "LISA Proposal for a Laser-Interferometer Gravitational Wave Detector in Space", unpublished proposal submitted to ESA in May 1993; available as document MPQ 177 from the Max-Plank-Institut für Quantenoptik, 8046 Garching bei München, Germany.
Einasto, J.E. 1979, in: The Large-Scale Characteristics of the Galaxy, IAU Symp. 84, Ed. W.B.Burton, D.Reidel: Dordrecht, p. 451.
Grishchuk, L.P. 1988, Uspekhi Fiz. Nauk 156, 297.
Hills, D.L., Bender, P. & Webbink, R.F. 1990, ApJ 360, 75.
Iben, I., Jr. & Tutukov, A.V. 1984, ApJSS 54, 335.
Lipunov, V.M. & Postnov, K.A. 1987, AZh 64, 438.
Lipunov, V.M., Postnov, K.A. & Prokhorov, M.E. 1987, A&A 176, L1.
Lipunov, V.M. & Postnov, K.A. 1988, ApSS 145, 1.
Lipunov, V.M., Postnov, K.A. & Prokhorov, M.E. 1994, in preparation.
Narayan, R., Piran, T. & Shemi, A. 1991, ApJ 379, L17.
Phinney, E.S. 1991, ApJ 380, L17.
Rubakov, V.A., Sazin M.V. & Veryaskin A.V. 1982, Phys. Lett. B 115, 189.
Sil'chenko, O.K. 1984, AZh 61, 74.
Smoot, G. et al., 1992, ApJ 396, L1.
Strukov, I.A. et al., 1993, Phys. Lett. B 315, 198.
Thorne, K.S. 1988, in: 300 Years of Gravitation, Eds. S.W.Hawking and W.Israel, Cambridge Univ. Press, p.330.
Thorne, K.S. 1994, in: Proc. of the Eight Nishinomiya-Yukawa Symp. on Relativistic Cosmology, Ed. M.Sasaki, Universal Academy Press, Japan, in press.
Tully, R.B. 1988, Nearby Galaxies Catalog. Cambridge Univ. Press.
Tutukov, A.V. & Yungelson, L.R. 1993, MNRAS 260, 675.

van den Bergh, S. & Tammann, G.A. 1991, ARA&A 29, 363.
van den Heuvel, E.P.J. 1994, in: Interacting Binaries, Eds. S.N.Shore, M. Livio and E.P.J. van den Heuvel, Springer: Berlin, chapter 3.
Webbink, R.F. 1979, in: White Dwarfs and Variable Degenerate Stars, IAU Colloq. 53, Eds. Van Horn, H.M., and Weidemann, V., Rochester Univ. Press, Rochester, p. 426.

This article was processed by the author using Springer-Verlag LaTeX A&A style file version 3.